

Optical properties of graphene nanoribbons: the role of many-body effects

Deborah Prezzi,^{1,2,*} Daniele Varsano,¹ Alice Ruini,^{1,2} Andrea Marini,³ and Elisa Molinari^{1,2}

¹*INFN-CNR-S3, National Center on nanoStructures and bioSystems at Surfaces, I-41100 Modena, Italy.*

²*Dipartimento di Fisica, Università di Modena e Reggio Emilia, I-41100 Modena, Italy.*

³*Dipartimento di Fisica, Università di Roma "Tor Vergata", I-0133 Roma, Italy.*

(Dated: October 22, 2018)

We investigate from first principles the optoelectronic properties of nanometer-sized armchair graphene nanoribbons (GNRs). We show that many-body effects are essential to correctly describe both energy gaps and optical response. As a signature of the confined geometry, we observe strongly bound excitons dominating the optical spectra, with a clear family dependent binding energy. Our results demonstrate that GNRs constitute 1D nanostructures whose absorption and luminescence performance can be controlled by changing both family and edge termination.

PACS numbers: 73.22.-f, 78.67.-n, 78.30.Na

Keywords:

Graphite-related nanoscale materials, such as fullerenes and nanotubes, have long been the subject of an intense research for their remarkable properties [1]. The recent discovery of stable, single-layer graphene [2, 3, 4] has prompted the attention on a different graphitic quasi-1D nanostructure, i.e. graphene nanoribbons (GNRs). These systems have been theoretically studied in the past decade [5, 6, 7, 8, 9] as simplified models of defective nanotubes and graphite nano-fragments. However, only very recently isolated nanometer-sized GNRs have been actually synthesized by etching larger graphene samples, or by CVD growth on suitably patterned surfaces [10, 11, 12]. The production techniques advanced in these pioneering works are expected to become highly controllable, opening up new avenues for both fundamental nanoscience and nanotechnology applications.

One of the most striking features of GNRs is the high sensitivity of their properties to the details of the atomic structure [5, 6, 7, 13, 14, 15, 16]. In particular, the edge shape dictates their classification in armchair (A), zigzag (Z) or chiral (C) ones, thus determining their energy band gaps. In addition to an overall decrease of energy gaps with increasing ribbon width, also observed experimentally [11], theoretical studies predict a superimposed oscillation feature [13, 14, 15], which is maximized for A-GNRs. According to this behaviour, A-GNRs are further classified in three distinct families, i. e. $N = 3p - 1$, $N = 3p$, $N = 3p + 1$, with p integer, where N indicates the number of dimer lines across the ribbon width. This fine sensitivity to the atomic configuration raise the opportunity to tailor the optoelectronic properties of A-GNRs by appropriately selecting both ribbon family and width.

In spite of this interest, previous theoretical studies of the electronic (see e.g. Refs. 6, 15, 16) and optical properties [14] of GNRs were only based on the independent-particle approximation or on semi-empirical calculations. However, many body effects are expected to play a key

role in low dimensional systems [17, 18, 19, 20, 21] due to enhanced electron-electron correlation. Motivated by this theoretical issue and by recent experimental progress [10, 11, 12] pursuing the potential of GNRs for nanotechnology applications, we have carried out *ab initio* calculations to study the effects of many-body interactions on the optical spectra of 1-nm-wide A-GNRs belonging to different families.

In this Letter, we show that a sound and accurate description of the optoelectronic properties of A-GNRs must include many-body effects. We will demonstrate that there are many signatures of the non-local correlations occurring in these confined systems. First of all, quasiparticle corrections are found to be strongly state-dependent. Moreover, the optical response of A-GNRs is dominated by prominent excitonic peaks, with a complex bright-dark structure which would not have been even expected from an independent-particle framework. Both quasi-particle corrections and exciton binding energies are found to exhibit an oscillating behaviour, according to the family classification. Finally, the electronic and optical properties of hydrogen passivated A-GNRs are compared with those of clean-edge ribbons: including many-body effects allows us to single out the impact of this edge modification on absorption and luminescence.

The first-principles calculation of the optical excitations is carried out using a many-body perturbation theory approach, based on a three-step procedure [22]. As a preliminary step, we obtain the ground state electronic properties of the relaxed system, by performing a density-functional theory (DFT) supercell calculation, within the local density approximation (LDA) [23, 24]. Second, the quasiparticle corrections to the LDA eigenvalues are evaluated within the G_0W_0 approximation for the self-energy operator, where the LDA wavefunctions are used as good approximations for the quasiparticle ones, and the screening is treated within the plasmon-pole approximation [25]. Third, the electron-hole interaction is included by solving the Bethe-Salpeter (BS) equation in

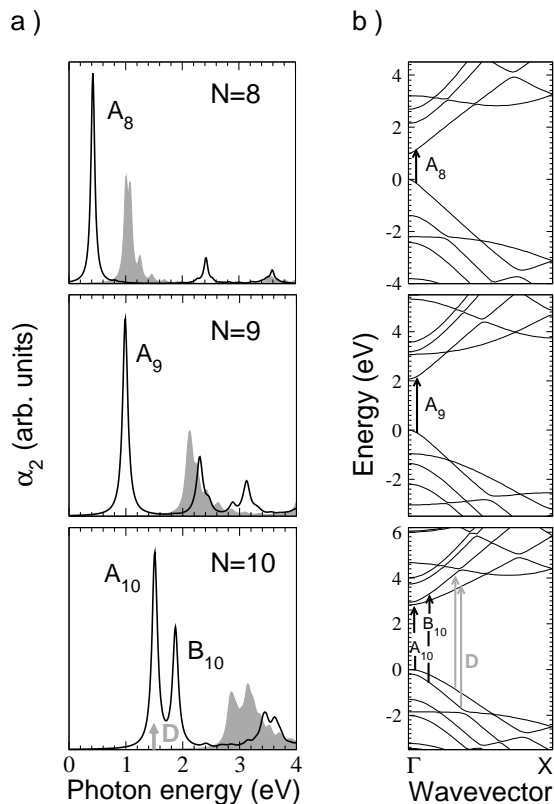


FIG. 1: (a) Optical absorption spectra of 1 nm wide hydrogen-passivated GNRs: $N = 8$ (1.05 nm wide), $N = 9$ (1.17 nm) and $N = 10$ (1.29 nm). In each panel, the solid line represents the spectrum with electron-hole interaction, while the spectrum in the single-particle picture is in grey. All the spectra are computed introducing a lorentzian broadening. (b) Quasiparticle bandstructures.

the basis set of quasidelectron and quasihole states, where the static screening in the direct term is calculated within the random-phase approximation (RPA). Only the resonant part of the BS hamiltonian is taken into account throughout the calculations (Tamm-Dancoff approximation), since we have verified that the inclusion of the coupling part does not affect significantly the absorption spectra [26]. Moreover, only the case of light polarized along the ribbon axis is examined, as a significant quenching of optical absorption is known to occur in 1D systems for polarization perpendicular to the principal axis [27]. All the *GW*-BS calculations are performed with the code SELF [28, 29].

To treat an isolated system in the supercell approach, we consider a separation of 40 a.u. between images in the directions perpendicular to the ribbon axis. Moreover, in both *GW* and BS calculations, we truncate the long-range screened Coulomb interaction between periodic images, in order to avoid non-physical interactions [30]. Due to the rectangular geometry of the system, we use a box-shaped truncation [31].

We start by considering 1 nm wide hydrogen-

passivated A-GNRs belonging to different families, namely $N = 8, 9, 10$. Figure 1 (a) depicts their calculated optical absorption spectra, while the quasiparticle bandstructures are shown in Fig. 1 (b). All the results are summarized in Table I. The quasiparticle *GW* corrections open the LDA energy gaps at Γ by 0.72, 1.32 and 1.66 eV for $N = 8, 9$ and 10, respectively. These energy corrections are larger than those of bulk semiconductor with similar LDA gaps, due to the enhanced Coulomb interaction in low dimensional systems. In addition, a family modulation of the corrections can be noticed, with larger corrections for the GNRs with larger LDA gaps. The gap opening is accompanied by an overall stretching of the bandstructure of 17 – 22%, similar to the value found for graphene (about 20%) [32].

In the absence of e-h interaction, such a bandstructure would result in the optical absorption spectra depicted in grey [Fig. 1 (a)], characterized by prominent 1-D van Hove singularities. The inclusion of the excitonic effects (solid black line) dramatically modifies both the peak position and absorption line-shape, giving rise to individual excitonic states below the onset of the continuum, with binding energy of the order of the eV.

The lowest-energy absorption peaks for $N = 8$ and 9, labelled A_8 and A_9 , have the same character: in both cases, the principal contribution comes from optical transitions between the last valence and first conduction bands, localized in *k*-space near the Γ point [Fig. 1 (b)]. The binding energies for these lowest optically active excitons are 0.58 and 1.11 eV for $N = 8$ and 9, respectively. As compared to the first two systems, the $N = 10$ GNR shows a richer low-energy spectrum. Each noninteracting peak gives rise to a bright excitonic state [arrows A_{10} and B_{10} in Fig. 1 (b)], with binding energies of 1.31 and 0.95 eV. In addition, the mixing of dipole forbidden transitions between the same bands [arrows D in Fig 1 (b)] is responsible for an optically inactive exciton degenerate in energy with A_{10} . The D state thus provides a competing path for non radiative decay of optical excitations, which could affect the luminescence yield of the system. This feature results from transitions between pairs of bands very close in energy to each other, and is therefore expected to be a common outcome for all $N = 3p+1$ GNRs.

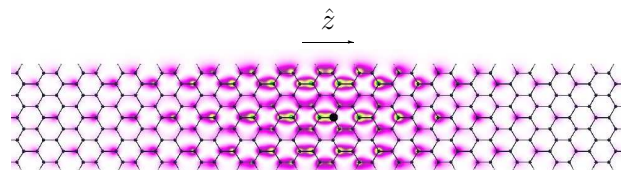


FIG. 2: In-plane spatial distribution of the electron for a fixed hole position (black dot), corresponding to the lowest excitonic peak in the $N = 9$ case. The spatial density is averaged over the direction orthogonal to the ribbon plane. Dimension of the panel: 1.2×6.4 nm.

N	LDA	GW	BS	E_b
8-H	0.28	1.00	0.42	0.58
8	0.50	1.59	0.71	0.88
9-H	0.78	2.10	0.99	1.11
9	0.56	1.50	0.64	0.86
10-H	1.16	2.82	1.51, 1.87	1.31, 0.95
10	1.09	2.64	1.46, 1.68	1.18, 0.96

TABLE I: Energy gap (2nd and 3rd columns) and peak position (4th column) for $N = 8, 9$ and 10 A-GNRs, with (-H) and without hydrogen passivation of the edge sites. The relative binding energies are reported in the last column. All the values are in eV.

A further insight in the effects of electron-hole interaction is provided by the evaluation of the resulting spatial correlations. In Fig. 2, we plot the in-plane probability distribution of the electron for a fixed hole position (black dot), corresponding to the lowest excitonic state in the $N = 9$ case. While the electron distribution extends over the whole ribbon width, the modulation of the exciton wavefunction $|\psi(\mathbf{r}_e; \mathbf{r}_h)|^2$ along the ribbon axis is entirely determined by the Coulomb interaction. Similar wavefunctions (not reported here) for the lowest excitons have been obtained for GNRs of different families, with spatial extensions [33] of about 34, 23 and 18 Å for $N = 8, 9$ and 10 , respectively.

We now consider the case of clean-edge nanoribbons, since this simple variation of the structure has been often suggested for ribbons obtained by high-temperature treatments or by dehydrogenation of hydrocarbons [8, 14, 34]. This analysis allows us to further explore the role played by edge effects in the optoelectronic properties. Our results are summarized in Fig. 3 and Table I. As expected, the hydrogen removal leads to a major edge reconstruction, with the appearance of carbyne-like structures. In fact, the bond length for the edge dimers reduces from 1.36 for the passivated ribbons to 1.23 Å for the clean ones, pointing to the formation of C-C triple bonds at the edges. This edge modification leads to a variation of the energy gaps, such that the distinction between $N = 3p - 1$ and $N = 3p$ families vanishes, in agreement with previous results [14].

In Fig. 3 (a), we report the quasiparticle bandstructure for the $N = 9$ bare ribbon. The main difference with respect to its passivated counterpart is the presence of edge-related bands (see arrows) in the low-energy optical window. Hence, we focus our attention on the properties of these edge states and their influence on the optical response. These states show the same energy dispersion and real-space localization, irrespective of both family and size, already in the LDA framework [35]: due to this independence on bulk properties, their presence is reasonably expected for all non-passivated ribbons. The self-energy corrections to the LDA eigenvalues are similar to those of the passivated systems for the π and π^* bulk

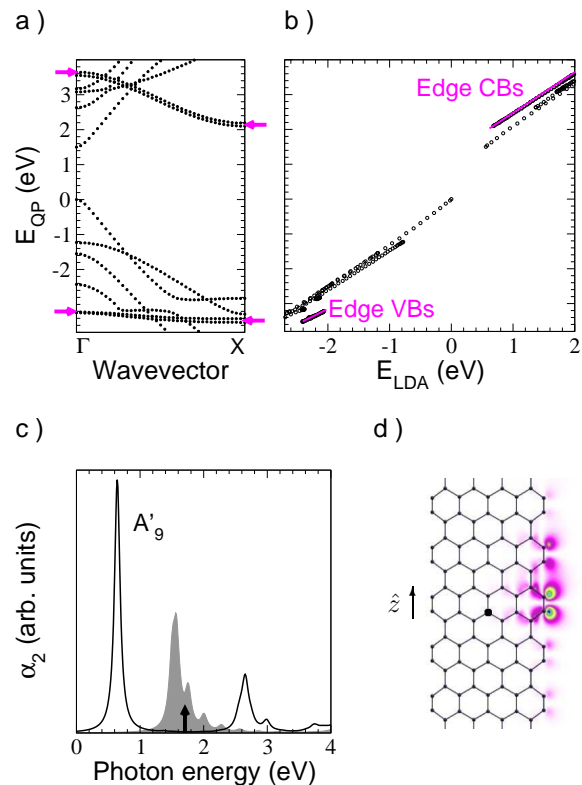


FIG. 3: (a) Quasiparticle bandstructure of the $N = 9$ hydrogen-free GNR. Arrows indicate the edge related single particle bands. (b) Plot of the GW quasiparticle energies vs the LDA energies. (c) Optical absorption spectrum, with (solid black) and without (grey) excitonic effects. The black arrow indicates the energy position of the optically forbidden edge-related exciton. Its excitonic wavefunction is depicted in panel (d), whose dimension is 1.0×2.2 nm.

states. The edge states show quite a different correction, being deeper in energy and with a smoothed stretching with respect to the other bands [Fig.3 (b)]. This behaviour is to be ascribed to the different degree of real-space localization between bulk and edge states, and it can be singled out by virtue of the non-local character of the self-energy operator in the GW framework, which is not correctly described within LDA.

The aforementioned modification of the bandstructure results in a correspondent blueshift ($N = 8$) or redshift ($N = 9$) of the lowest excitonic peak, with A'_8 and A'_9 becoming almost degenerate, with binding energies of about 0.9 eV. For the case of $N = 10$, we find an inversion of the first and second conduction bands, which results in the B'_{10} peak lying below A'_{10} and D' almost degenerate in energy with B'_{10} . In addition, the edge states introduce an optically inactive exciton, which arises from transitions among several bulk valence bands and the conduction edge states over the whole Brillouin zone. This *edge exciton* is present in all the studied nanoribbons and is located at about 1.4-1.7 eV (black arrow in Fig 3 (d)),

with very little dependence on family and size [35]. This results in the edge exciton being above the first excitonic peak for $N = 8$ and 9, and between the first and the second peaks for $N = 10$. We remark that the accurate evaluation of quasi-particle corrections within *GW*, i.e. beyond the usual approximation based on a uniform band stretching on top of a rigid energy shift, is crucial to determine the exact energy position of the dark edge excitons relative to the bright ones.

To better understand the character of the edge-related dark state, we plot its excitonic wavefunction for the case $N = 9$ in Fig. 3 (d). The mixing of transitions over the whole Brillouin zone induces a strong localization of the edge exciton along the ribbon axis, with an extent of only ~ 5 Å, that is 4-7 times smaller than the Wannier-like *bulk excitons* (see Fig. 2).

In summary, we have found that the analysis of the electronic and optical features of GNRs requires a state-of-the-art approach within the many-body perturbation theory, and beyond the DFT framework. Many-body effects reveal that nanosized A-GNRs retain a quasi-1D character, which induces the suppression of the van Hove singularity, typical of non-interacting 1D systems, and the appearance of strong excitonic peaks in the optical absorption spectrum. The lowest excited states in GNRs are Wannier-like excitons and their binding energy as well as their luminescence properties are strongly dependent on the ribbon family. We investigate the role of many-body effects on the edge-states arising in non-passivated GNRs: our analysis could provide a practical tool for revealing the nature of the edges in realistic samples. We demonstrate that GNRs are intriguing systems with tunable optoelectronic features, that we quantitatively evaluate through our calculations. The present study calls for experiments addressing the optical response of GNRs: A combined theoretical and experimental understanding of ribbon size, family and edge-termination as control parameters for their performance can be considered as the first step towards the design of graphene-based applications in nanoscale optoelectronics.

We are grateful to A. Rubio, A. C. Ferrari, S. Piscanec, B. Montanari, T. Weller, M. Rontani and C. Cavazzoni for stimulating discussions. We acknowledge CINECA CPU time granted through INFN-CNR. D. V. and A. M. thank the European Nanoquanta NoE (NMP4-CT-2004-500198) and the European Theoretical Spectroscopy Facility (ETSF).

* corresponding author: prezzi.deborah@unimore.it

- [1] G. Dresselhaus, M. S. Dresselhaus, and P. C. Eklund, editors, *Science of Fullerenes and Carbon Nanotubes: Their Properties and Applications*, Academic, New York, 1996.
- [2] K. S. Novoselov et al., *Nature (London)* **438**, 197 (2005).

- [3] Y. Zhang, Y.-W. Tan, H. L. Stormer, and P. Kim, *Nature (London)* **438**, 201 (2005).
- [4] C. Berger et al., *Science* **312**, 191 (2006); C. Berger et al., *J. Phys. Chem. B* **108**, 19912 (2004).
- [5] M. Fujita, K. Wakabayashi, K. Nakada, and K. Kusakabe, *J. Phys. Soc. Jpn.* **65**, 1920 (1996).
- [6] K. Nakada, M. Fujita, G. Dresselhaus, and M. S. Dresselhaus, *Phys. Rev. B* **54**, 17954 (1996).
- [7] K. Wakabayashi, M. Fujita, H. Ajiki, and M. Sigrist, *Phys. Rev. B* **59**, 8271 (1999).
- [8] T. Kawai, Y. Miyamoto, O. Sugino, and Y. Koga, *Phys. Rev. B* **62**, R16349 (2000).
- [9] K. Kusakabe and M. Maruyama, *Phys. Rev. B* **67**, 092406 (2003).
- [10] Z. Chen, Y.-M. Lin, M. J. Rooks, and P. Avouris, *Cond-Mat*, 0701599 (2007).
- [11] M. Y. Han, B. Ozyilmaz, Y. Zhang, and P. Kim, *Cond-Mat*, 0702511 (2007).
- [12] T. Tanaka et al., *Solid State Commun.* **123**, 33 (2002).
- [13] M. Ezawa, *Phys. Rev. B* **73**, 045432 (2006).
- [14] V. Barone, O. Hod, and G. E. Scuseria, *Nano Lett.* **6**, 2748 (2006).
- [15] Y.-W. Son, M. L. Cohen, and S. G. Louie, *Phys. Rev. Lett.* **97**, 216803 (2006).
- [16] L. Pisani, J. A. Chan, B. Montanari, and N. M. Harrison, *Phys. Rev. B* **75**, 064418 (2007).
- [17] A. Ruini, M. J. Caldas, G. Bussi, and E. Molinari, *Phys. Rev. Lett.* **88**, 206403 (2002).
- [18] M. Rohlfing and S. G. Louie, *Phys. Rev. Lett.* **82**, 1959 (1999).
- [19] E. Chang, G. Bussi, A. Ruini, and E. Molinari, *Phys. Rev. Lett.* **92**, 196401 (2004).
- [20] C. D. Spataru, S. Ismail-Beigi, L. X. Benedict, and S. G. Louie, *Phys. Rev. Lett.* **92**, 077402 (2004).
- [21] M. Bruno, M. Palumbo, A. Marini, R. Del Sole, and S. Ossicini, *Phys. Rev. Lett.* **98**, 036807 (2007).
- [22] For a recent review see, e.g., G. Onida, L. Reining, and A. Rubio, *Rev. Mod. Phys.* **74**, 601 (2002).
- [23] S. Baroni, A. Dal Corso, S. de Gironcoli, and P. Gianozzi, 2001, <http://www.pwscf.org>.
- [24] The DFT-LDA calculations are carried out using separable norm-conserving pseudopotentials and a plane-wave basis set. A kinetic energy cutoff of 50 Ry is employed. Each atomic structure has been fully relaxed, until forces acting on atoms were less than 0.01 eV/Å. The relaxed configurations are always planar, for both passivated and clean-edge structures.
- [25] R. W. Godby and R. J. Needs, *Phys. Rev. Lett.* **62**, 1169 (1989).
- [26] We have calculated the excitation energies with and without the inclusion of the coupling part for few cases and always found differences well below our computational accuracy (0.1 eV).
- [27] A. G. Marinopoulos, L. Reining, A. Rubio, and N. Vast, *Phys. Rev. Lett.* **91**, 046402 (2003).
- [28] A. Marini et al., the SELF project, <http://www.fisica.uniroma2.it/~self/>.
- [29] All *GW*-BS calculations have been converged with respect to the number of conduction bands, the k-points sampling, the cutoff on local field effects, until errors were less than 0.1 eV.
- [30] C. A. Rozzi, D. Varsano, A. Marini, E. K. U. Gross, and A. Rubio, *Phys. Rev. B* **73**, 205119 (2006).
- [31] D. Varsano and A. Marini, 2007, unpublished.

- [32] C. Attacalite, L. Wirtz, and A. Rubio, private comm.; A. Grueneis et al., unpublished.
- [33] We calculate the extension as the full width at half maximum of the probability distribution.
- [34] L. R. Radovic and B. Bockrath, *J. Am. Chem. Soc.* **127**, 5917 (2005).
- [35] We check the results for few other cases up to 2 nm.